

Estimating the pattern of synchrony in fluctuating populations

STEINAR ENGEN*, RUSSELL LANDE†, BERNT-ERIK SÆTHER‡
and THOMAS BREGNBALLE§

*Department of Mathematical Sciences, Norwegian University of Science and Technology, N-7491 Trondheim, Norway; †Department of Biology 0116, University of California – San Diego, La Jolla, CA 92093, USA; ‡Department of Zoology, Norwegian University of Science and Technology, N-7491-Trondheim, Norway; and §National Environmental Research Institute, Department of Coastal Zone Ecology, Kalø, Grenåvej 12, DK 8410 Rønde, Denmark

Summary

1. A central question in population ecology is how to estimate the effects of common environmental noise, e.g. due to large-scale climate patterns, on the synchrony in population fluctuations over large distances. We show how the environmental variance can be split into components generated by several environmental variables and how these can be estimated from time-series observations.

2. With a set of time-series observations from different locations not necessarily covering the same time span, it is shown how the spatial autocorrelation of the residual variance component, not explained by the covariates and corrected for demographic stochasticity, can be estimated using classical multinormal theory.

3. Some previous results on spatial scaling in continuous linearized models on log scale are extended to also provide the scaling for the residuals. This is shown to be close to the spatial scaling of the autocorrelation in the environmental noise and only weakly affected by migration.

4. The logistic model of local population dynamics with the NAO index as the only covariate is fitted to 22 populations of the Continental great cormorant *Phalacrocorax carbo sinensis*. The spatial scale of the environmental noise is estimated to be about 155 km. The NAO index alone accounts for about 10% of the total environmental variance and nearly all of the regional environmental variance (long-distance environmental autocorrelation).

Key-words: environmental stochasticity, spatial ecology, Moran effect, spatial scaling.

Journal of Animal Ecology (2005) **74**, 601–611

doi: 10.1111/j.1365-2656.2005.00942.x

Introduction

Vertebrate populations often show synchronous population fluctuations in space. It has been well known for several decades (Elton 1924) that the populations of some species such as the snowshoe hare (*Lepus americanus*) or the arctic lemming (*Lemmus norvegicus*) in many areas show similar fluctuations at sites separated by hundreds of kilometres (Stenseth *et al.* 1999). Recently, comparative analysis involving several species living in the same area have in general demonstrated large inter-

specific variation, even among closely related species, in the spatial scaling of the synchrony in population fluctuations (Lindström, Ranta & Lindén 1996; Paradis *et al.* 1999, 2000; Cattadori, Merler & Hudson 2000). We still do not understand the mechanisms generating such interspecific differences in synchrony.

Analyses of linear or log-linear models have shown that the autocorrelation in the fluctuations in log size of two populations with no migration between them equals the autocorrelation in the environmental noise (Moran 1953; Lande, Engen & Sæther 1999). This also applies for between-years changes in log population sizes. Some evidence suggests that such a Moran effect can synchronize population fluctuations (Grenfell *et al.* 1998). Lande *et al.* (1999), Bjørnstad & Bolker (2000), Kendall *et al.* (2000), Ripa (2000), Engen (2001) and

Correspondence: Steinar Engen, Department of Mathematical Sciences, Norwegian University of Science and Technology, N-7491 Trondheim, Norway. Fax: +47 72 55 33 14; E-mail: steinaen@math.ntnu.no

Engen, Lande & Sæther (2002a,b) extended these results to also include migration and showed that even short-distance migration may contribute substantially to an increase in the scale of population synchrony, especially if population-density regulation is weak. Extensive simulation studies of discrete time models have supported these results (Ranta, Kaitala & Lundberg 1997b; Ranta, Lindström & Helle 1997a). Thus, these analyses demonstrate that factors affecting environmental variation in space and time as well as processes acting within the populations themselves (e.g. strength of density regulation) influence the strength and scaling of synchrony in population fluctuations. Geographical patterns in population fluctuations often are studied using the Mantel test (Koenig 1999). Two matrices are computed: a distance matrix of the distances between all possible pairs of sites and a correlation matrix where the elements are the correlation coefficients of annual variation in population sizes at all possible pairs of study sites. A standard way to present the data is to plot the correlation coefficient computed from pairs of time-series observed during the same period against the distance between the different pairs of study plots. How rapidly the correlation decreases with distance indicates the spatial scaling of the synchrony in the population fluctuations. Although several modifications of this method have been suggested (Bjørnstad, Stenseth & Saitoh 1999a; Peltonen *et al.* 2002), a major problem with these non-parametric approaches is to link theory with data (Bjørnstad, Ims & Xavier 1999b). Another problem with the kind of non-parametric approach described above is that demographic stochasticity in population fluctuations is not taken into account. Demographic stochasticity is dominating compared to environmental stochasticity when local populations are small (Lande, Engen & Sæther 2003), and has by definition (Engen, Bakke & Islam 1998) no spatial scaling. Consequently population synchrony, which can only be affected by environmental stochasticity, is expected to increase with population size.

Here we provide a model that utilizes knowledge about the demographic variance and incorporates the possibility of a decrease of synchrony with population size due to demographic stochasticity. Our approach is especially useful for fully censused populations in which we can ignore sampling errors in population estimates and work with the full likelihood function for the problem. One advantage of this, in addition to the possibility of including demographic stochasticity, is that we can include any observed population size in the analysis and do not need to pay attention to the fact that the time-series only partly overlap in time. Rather than using raw estimates of correlations we work directly with the likelihood function using the complete set of residuals obtained after fitting models to the local populations.

The correlations then enter the model through the parameters of a spatial autocorrelation function. A third advantage with our approach is that we can

assume that the local populations possibly have different dynamics. We do this by fitting stochastic population models to each local population, and include in the spatial analysis only the environmental component of the residuals, correcting for expected change in population size for different values of population sizes the previous year. Because theoretical as well as empirical analyses have focused previously on the synchrony of (log) population sizes or between years change in (log of) these (see Ranta *et al.* 1997b and Bjørnstad *et al.* 1999), we also include a theoretical analysis of the spatial scaling of residuals in a continuous homogeneous model in space and time with migration.

We apply this method to estimate the pattern of synchrony in the fluctuations of breeding populations of the Continental Great Cormorant *Phalacrocorax carbo sinensis* in Europe. We focus especially on how a large-scale climate phenomenon, the North Atlantic Oscillation (Hurrell *et al.* 2003), affects the spatial scaling of population synchrony.

Methods

SINGLE LOCATION ANALYSIS

Writing N_t for the population size at a given location, the dynamics are modelled by:

$$N_{t+1} = N_t + r_t N_t - g(N_t) \quad \text{eqn 1}$$

where r_t is the growth rate varying stochastically between years and $g(\cdot)$ is an increasing function defining the local density regulation. For population fluctuations driven by demographic and environmental stochasticity we have $\text{var}(r_t) = \sigma_e^2 + \sigma_d^2/N_t$ where σ_e^2 and σ_d^2 are the environmental and demographic variance, respectively (May 1973, 1974; Turelli 1977; Engen *et al.* 1998; Lande *et al.* 2003). The demographic variance can be estimated by a simple sum of squares from individual data on survival and reproduction (Sæther *et al.* 1998; Lande *et al.* 2003). When such data are available, one will usually have data from a large number of individuals, giving accurate estimates of the demographic variance (Sæther *et al.* 1998). In the following we therefore consider the demographic variance to be known. We shall use the logistic form of density regulation, $g(N) = \beta N^2$. Then, for small and moderate population fluctuations a simple first-order approximation gives the model:

$$E(\ln N_{t+1} | N_t) = \ln N_t + \bar{r} - \frac{1}{2} \sigma_e^2 - \frac{1}{2N_t} \sigma_d^2 - \beta N_t \quad \text{eqn 2}$$

and

$$\text{var}(\ln N_t | N_t) = \sigma_e^2 + \sigma_d^2/N_t$$

(Lande *et al.* 2003).

The model may alternatively be written

$$X_{t+1} = E(X_{t+1} | X_t) + U_d \sigma_d / \sqrt{N_t} + U_e \sigma_e \quad \text{eqn 3}$$

where $X_t = \ln N_t$ while U_d and U_e are independent variables with zero mean and unit variance. Our main goal is to investigate the environmental noise terms $U_e\sigma_e$ at different locations, including the population synchrony it generates. The temporal and spatial stochastic fluctuations in this term may be generated partly by other quantities such as, for example, the local abundance of other species, the local temperature and the NAO index. We introduce such quantities generally as random effects writing:

$$U_e\sigma_e = \sum \alpha_i y_{i,t} + U\sigma, \tag{eqn 4}$$

where $y_{i,t}$ is the above random covariate number i at time t , U is another normalized variable and σ^2 is the component of the environmental variance that can not be explained by fluctuations in the covariates. This leads to the relation $\sigma_e^2 = \text{var}(\sum \alpha_i y_{i,t}) + \sigma^2$, so that the covariates together explain a fraction:

$$p = \text{var}(\sum \alpha_i y_{i,t}) / \text{var}[(\sum \alpha_i y_{i,t}) + \sigma^2] \tag{eqn 5}$$

of the total environmental variance. This decomposition of the environmental variance is also valid if the covariates are subject to noise with temporal autocorrelation. In this case the total environmental noise term U_e may also have a temporal autocorrelation. However, this does not affect our approach, which only assumes that the residual noise term obtained after correcting for the effect of the covariates is generated by a white noise process.

Assuming that $X_{t+1} = \ln N_{t+1}$ is normally distributed when conditioned on N_t , and writing $f(x; \mu, \sigma^2)$ for the normal probability distribution with mean μ and variance σ^2 , the log likelihood function takes the form:

$$\ln L = \sum \ln f(X_{t+1}; m(N_t, Y_t), v(N_t)), \tag{eqn 6}$$

where Y_t denotes the vector of covariates, $v(N) = \sigma^2 + \sigma_d^2/N$, and the mean is the appropriate modification of eqn 2:

$$m(N_t; y_t) = \ln N_t + \bar{r} - \frac{1}{2} \sigma_e^2 - \frac{1}{2N_t} \sigma_d^2 - \beta N_t + \sum \alpha_i y_{i,t} \tag{eqn 7}$$

The sum in eqn 6 is taken over those years for which the population size in the previous year is known. This means that if there are time gaps in the data of more than one year, we ignore the information contained in the population change over this gap, which in any case will be small.

Now, assuming known demographic variance, all other unknown parameters are estimated by numerical maximization of log likelihood, and uncertainties are evaluated by parametric bootstrapping involving simulating the time-series using the initial population size and the estimated parameters.

SPATIAL ANALYSIS

The spatial analysis will be based on studying the residuals obtained from fitting the model to time-series observations at each location z ,

$$R_{t+1}(z) = X_{t+1}(z) - \hat{E}[X_{t+1}(z) | X_t(z), Y_t] \approx \sigma(z)U(z) + \sigma_d(z)U_d(z)/\sqrt{N(z)}, \tag{eqn 8}$$

where \hat{E} denotes the estimated expected value. We use the normal approximation and choose a parametric form for the spatial autocorrelation of the U , of the form:

$$\rho(z) = \text{corr}[U(w), U(w+z)] = \rho_\infty + (\rho_0 - \rho_\infty)h(z), \tag{eqn 9}$$

where $h(z)$ decreases from 1 to 0 as z increases from 0 to infinity. We use the exponential function $h(z) = e^{-z/l}$ and the Gaussian form $h(z) = e^{-z^2/(2l^2)}$ which both correspond to positive definite autocorrelation functions. Using the same type of spatial autocorrelation function for the population sizes, Lande *et al.* (1999) and Engen *et al.* (2002a,b) applied the standard deviation of the function $h(z)$ scaled to become a distribution as a measure of spatial scaling of population synchrony. Hence, the parameter l in the above functions is actually this measure of spatial scaling defined for the residuals.

Data from different locations often are available over different but partly overlapping time periods. However, for each year we do have a set of residuals with zero means, estimated standard errors, and correlations defined by eqns 8 and 9. For locations z_1 and z_2 the correlation is:

$$\text{corr}[R(z_1), R(z_2)] = \frac{\sigma(z_1)\sigma(z_2)\rho(z)}{\sqrt{[\sigma(z_1)^2 + \sigma_d(z_1)^2/N(z_1)][\sigma(z_2)^2 + \sigma_d(z_2)^2/N(z_2)]}} \tag{eqn 10}$$

For a given set of parameters (ρ_0, ρ_∞, l) defining the spatial synchrony, we have a complete description of a multivariate normal distribution each year, but possibly with different sets of locations at different years. The complete likelihood function is found by multiplying together the functions for each year or actually adding the log likelihood contributions for each year. Finally, this is maximized numerically to give estimates for (ρ_0, ρ_∞, l) . Generally, the more the time-series overlap, the more information the likelihood function contains about the correlation parameters (ρ_0, ρ_∞, l) . In order to obtain any information at all, we must require that at least two of the series are observed at least at one common time step. Otherwise the correlation parameters will be absent from the likelihood function and hence cannot be estimated.

The sampling properties of the estimates are found by parametric bootstrapping (Efron & Tibshirani 1993), that is, by simulating the whole set of local time-series, using the initial values of the data and the estimated parameters. The residuals must be simulated from the appropriate multinormal model defined by the autocorrelation function and the distance matrix.

The multinormal likelihood function can easily be calculated numerically using a lower triangular linear transformation, the Choleski decomposition (Ripley 1987). The same representation also gives a fast method for stochastic simulations required to perform the bootstrapping. This is explained in detail in Appendix I.

In Appendix II we extend some previous results for the scaling of spatial autocorrelation functions in a model that is linearized on the log scale. Lande *et al.* (1999) showed that the scaling for the population size defined as the above standard error derived from the autocorrelation, in a linear model allowing small and moderate fluctuations, was $l^2 = l_c^2 + ml_p^2/\gamma$. Here l_c is the scaling for the environmental noise, l_p^2 is the variance of the migration distance in a given direction (the p indicates the distribution of migration distance), m is the migration rate and γ is the strength of local density regulation. Engen (2001) derived the same result for a similar model on the log scale that allowed large population fluctuations, but with continuous migration modelled as a diffusion with l_p approaching zero and m approaching infinity keeping $ml_p^2 = M$. Engen *et al.* (2002b) showed for the same model that the scaling of the autocorrelation for the yearly differences of the log population sizes was close to $l_c^2 + M/2$ for $\gamma < 1$. Using the same model and the same approach it is shown in Appendix II that the scaling for the residuals in this model is:

$$l_R^2 = l_c^2 + M \left\{ 1/\gamma - \frac{2(1-\gamma)}{[1+(1-\gamma)^2]e^\gamma - 2(1-\gamma)} \right\} \text{ eqn 11}$$

which turns out to be close to $l_c^2 + M$ for $\gamma < 1.15$. Expressed by the mean yearly migration distance \bar{d} , this is approximately $l_c^2 + 0.64\bar{d}^2$.

Results

Two subspecies of great cormorant breed in Europe: the Atlantic great cormorant *P. c. carbo* and the continental great cormorant *P. c. sinensis*.

Their breeding ranges are mainly non-overlapping (Van Eerden, Koffijberg & Platteuw 1995), although in some areas individuals of both subspecies are found where they may even form mixed subspecies colonies (Carss & Ekins 2002). After the decline in persecution during the 1960s and 1970s, a rapid increase in numbers of continental great cormorant occurred (Van Eerden & Gregersen 1995), whereas in recent decades a decline in the rate of increase has been recorded over large parts of its breeding range (Bregnballe *et al.* 2003). We extracted censuses of fluctuations in the size of colonies of the continental great cormorant in Sweden and in continental Europe (Fig. 1). The colonies are censused by counting the number of active nests. The breeding habits of this species make it likely that inaccuracy in the population estimates is small. Only colonies that were censused for 15 or more years were included, in order to avoid large uncertainty in the parameters that were estimated separately for each location.

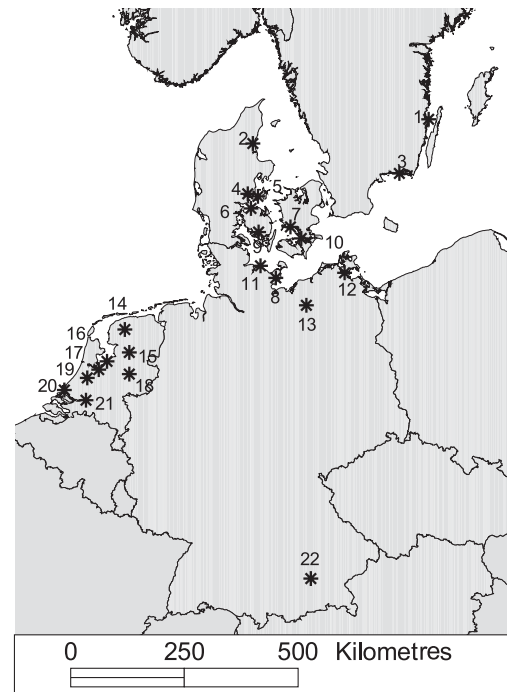


Fig. 1. Location of the study areas. The names are found in Table 1.

Large-scale changes in climate such as the North Atlantic Oscillation (NAO) have been found to affect the population dynamics of several marine vertebrates (Ottersen *et al.* 2001; Stenseth *et al.* 2002; Drinkwater *et al.* 2003), and can therefore contribute to the synchronization of population fluctuations over large areas. We analysed this effect using eqn 5 to investigate the extent to which variation in the NAO-index (<http://www.cgd.ucar.edu/cas/catalog/climind>) can explain variation in the annual change in size of the different populations.

The NAO-index is based on the difference of normalized sea level pressures (SLP) between Ponta Delgada, Azores, Portugal and Stykkisholmur, Iceland from 1864 to 2002 for the winter period December–March (Hurrell 1995). The NAO is a global climate phenomenon (Visbeck *et al.* 2001; Hurrell *et al.* 2003). In general, high values of NAO are associated with strong wind circulation in the North Atlantic causing an increase in temperatures and precipitation in northern Europe, but dry weather in the Mediterranean region (Hurrell 1995; Mysterud *et al.* 2000). In contrast, negative values of NAO are associated with decrease in temperature and precipitation in north-western Europe (Hurrell 1995; Mysterud *et al.* 2000; Catchpole *et al.* 2000).

The demographic variance was estimated from data on individual variation among females in their fitness contributions to the following generations in the population at Vorskø in Denmark (Fig. 1) using methods in Engen *et al.* (2005) for age-structured populations assuming age of maturity to be 2 years (Frederiksen & Bregnballe 2001). This is a well-studied colony where 12 024 chicks have been colour-ringed during the period

1977–2000 (see Frederiksen & Bregnballe 2000 and Schjørring, Gregersen & Bregnballe 2000 for further description). The estimation method is of the same type as the method used for estimating environmental variances in age-structured populations (Tuljapurkar 1982; Lande & Orzack 1988; Engen *et al.* 2005), except that the variances in vital rates are the within-years variation among individuals in survival and reproduction (see further description of estimation methods in Sæther *et al.* 2004; Engen *et al.* 2005). These variances are approximately inversely proportional to the total population size, and the constant factor of proportionality is the demographic variance of the process. This estimate is typical for bird species with age of maturity at 2–3 years (Lande *et al.* 2003; Sæther *et al.* 2004). We subsequently assume that this represents the demographic variance in all colonies.

An examination of the population estimates showed large intercolony variation in specific growth rate, ranging from 0.11 to 1.41 (Table 1). As the rate of return to K in the logistic model is equal to r (Lande *et al.* 2003), this also shows that the strength of density regulation around the carrying capacity differs among the colonies, although the uncertainty in the estimates of both those parameters was often large (Table 1).

Variation in NAO explained a significant proportion of the annual variation in the change in population size of 14 colonies (Table 1). All together, β_{NAO} was positive in 16 of 22 colonies. On average, variation in NAO explained 9.3% of the environmental variance σ_e^2 , ranging from 0 to 63%.

To examine the strength and scaling of the synchrony in the population fluctuations we fitted spatial autocorrelation functions of the Gaussian and exponential forms. Both models gave similar results (Fig. 2). For instance, at a distance of 5 km the correlation coefficient of the residuals was 0.197 and 0.225 in the Gaussian and the exponential models, respectively. Furthermore, the estimated scale of the local component of synchrony in the population fluctuations was 159 km for the Gaussian and 152 km for the exponential model. Parametric bootstrap distributions of the estimated scale are shown in Fig. 3. Although the estimated scale is uncertain, we do find the order of magnitude, and can conclude that the scale is smaller than about 300 km. As expected from Table 1, variation in NAO explained a proportion of the synchrony in the population fluctuations. We see that the NAO increases the autocorrelations of the environmental part of the residuals equally at all distances (Fig. 2) as it induces a common covariance between any residuals. The long-distance spatial autocorrelation is small, and seems to be mainly an effect of a synchronization of population fluctuations generated by fluctuations in the NAO index.

Discussion

Spatial autocorrelation in environmental noise as well as migration (Lande *et al.* 1999, 2003) and environmental heterogeneity (Engen *et al.* 2002b) will generate spatial autocorrelation in population fluctuations. This population synchrony can be observed for the total (log)

Table 1. The estimated parameters (\pm SD) for the different colonies of the cormorant. r is the specific growth rate and K is the carrying capacity, assuming a logistic model for the density regulation, β_{NAO} the regression coefficient of change in population size on NAO, σ_{NAO}^2 is the component of the environmental stochasticity explained by variation in NAO, σ_{res}^2 is the residual component unexplained by NAO and σ_e^2 is the total environmental variance. The figures in brackets refer to the location in Fig. 1

Locality	r	K	β_{NAO}	σ_{NAO}^2	σ_{res}^2	σ_e^2
Svartö (1)	0.37 \pm 0.12	1972 \pm 227	0.01	0.001	0.023	0.023 \pm 0.007
Toft Sø (2)	0.66 \pm 0.14	3178 \pm 605	-0.01	0.000	0.167	0.167 \pm 0.053
Fröstensskärv (3)	0.88 \pm 0.12	1422 \pm 130	-0.02	0.001	0.056	0.057 \pm 0.020
Vorsø (4)	0.11 \pm 0.04	4113 \pm 10566	0.02*	0.002	0.029	0.031 \pm 0.006
Svanegrund (5)	1.06 \pm 0.13	1260 \pm 100	-0.02	0.001	0.079	0.080 \pm 0.027
Mågeøerne (6)	0.81 \pm 0.11	2048 \pm 135	0.00	0.000	0.034	0.034 \pm 0.011
Ormø (7)	0.38 \pm 0.08	3698 \pm 621	0.04	0.006	0.055	0.061 \pm 0.016
Culpiner See (8)	0.58 \pm 0.17	416 \pm 60	0.02	0.002	0.087	0.089 \pm 0.029
Brændegård (9)	0.27 \pm 0.07	4992 \pm 956	0.04**	0.008	0.019	0.027 \pm 0.007
Dyrefod (10)	0.69 \pm 0.11	1453 \pm 91	0.05***	0.008	0.017	0.025 \pm 0.008
Selenter See (11)	0.87 \pm 0.18	303 \pm 49	0.03	0.004	0.242	0.246 \pm 0.079
Niederhof (12)	0.19 \pm 0.06	2411 \pm 3955	0.03	0.004	0.068	0.072 \pm 0.014
Bolzer See (13)	0.22 \pm 0.10	679 \pm 493	0.02	0.001	0.075	0.077 \pm 0.020
Princehof (14)	0.87 \pm 0.12	778 \pm 62	0.02	0.001	0.044	0.045 \pm 0.015
Bakkerskooi (15)	0.28 \pm 0.10	961 \pm 227	0.02	0.002	0.020	0.022 \pm 0.007
Oostvaardersplassen (16)	0.75 \pm 0.12	5887 \pm 479	0.04	0.007	0.058	0.065 \pm 0.018
Naardermeer (17)	0.18 \pm 0.14	3248 \pm 641	-0.01	0.001	0.027	0.028 \pm 0.007
Hengforden (18)	0.53 \pm 0.21	117 \pm 55	-0.07	0.026	0.170	0.196 \pm 0.074
Nieuwkoopse (19)	0.36 \pm 0.16	139 \pm 377	0.03	0.002	0.125	0.127 \pm 0.049
Brede Water (20)	1.41 \pm 0.13	1252 \pm 56	0.02	0.002	0.045	0.047 \pm 0.016
Dordtsche Biesbosch (23)	0.66 \pm 0.20	243 \pm 56	-0.03	0.003	0.340	0.343 \pm 0.101
Ismaninger Speichersee (24)	0.44 \pm 0.08	123 \pm 11	0.04***	0.010	0.006	0.016 \pm 0.006

* $P < 0.05$, ** $P < 0.01$, *** $P < 0.001$.

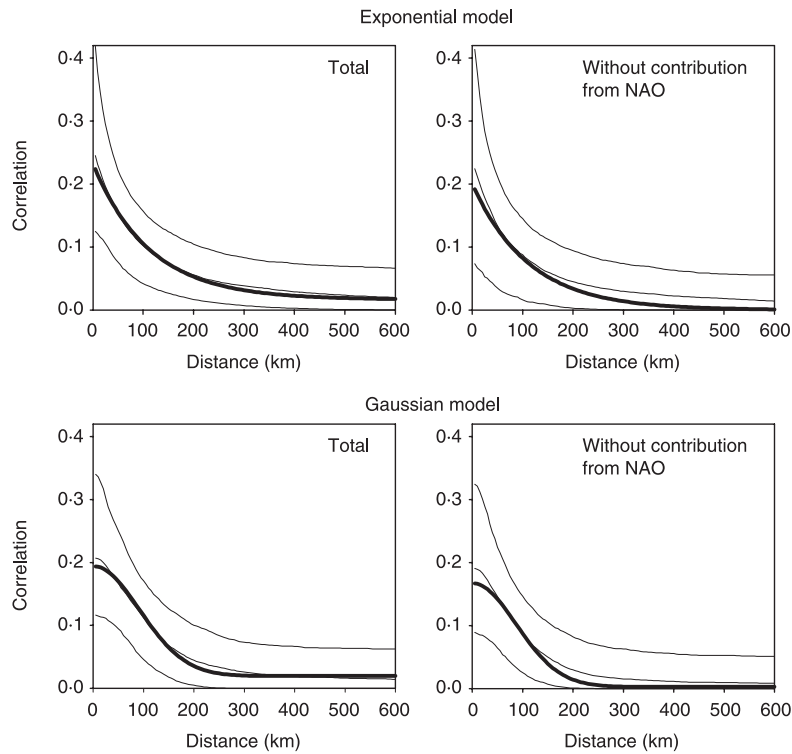


Fig. 2. The synchrony of fluctuations in population size in relation to distance for the exponential and Gaussian models. The thick line indicates the maximum likelihood estimate of the correlation coefficient, whereas the thin lines represent the 10%, 50% and 90% quantiles in the bootstrap distributions.

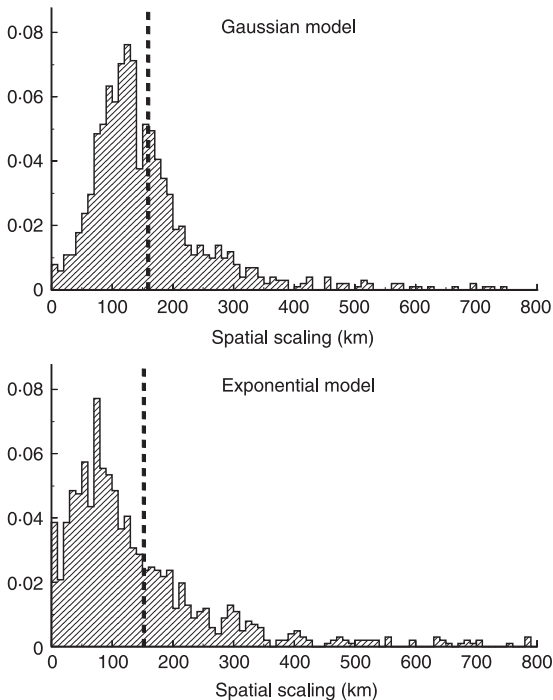


Fig. 3. Parametric bootstrap distribution for the estimate of spatial scaling based on assuming spatial autocorrelation functions of the exponential and Gaussian types. The dotted lines represent the estimated values.

work with the residuals measured at each location after fitting a stochastic population model. We use the local estimates for environmental variances and correct for the demographic component which, by definition, has no spatial autocorrelation. Analytical results have been derived previously to describe how migration and local density regulation affect the synchrony of (log) population size in continuous models (Lande *et al.* 1999; Bjørnstad & Bolker 2000; Engen 2001; Engen *et al.* 2002a,b), as well as discrete time models (Kendall *et al.* 2000; Ripa 2000). Many of these results have been supported qualitatively by simulation studies (Ranta *et al.* 1997a,b; Ranta *et al.* 1998). An important lesson from these analyses is that the scale of population synchrony depends on which characteristic of the population fluctuations is compared. In general, migration has greater effect on the scale of the fluctuations in population size than the scale of the yearly differences in population size, which is close to the scale of the local environmental noise (Engen *et al.* 2002a,b; Lande *et al.* 2003). Here we extend these results to show that the scale of the residuals also is close to that of the environmental noise. The effect of migration is approximately twice as large as that obtained using differences, but still small unless in cases where the spatial scale of the environmental noise can be neglected ($l_e \approx 0$).

Several approaches have been used to analyse spatial patterns of population fluctuations. One approach (Bjørnstad *et al.* 1999; Peltonen *et al.* 2002) is to calculate the correlations (parametric or non-parametric) between (log-) population size or yearly differences for each pair

population size and the yearly differences in (log of) these. In the present study we use the full likelihood function to estimate population synchrony. Because the dynamics differ among locations it is convenient to

of locations, using the time span where observations are available for both populations. A spatial autocorrelation function is then computed by smoothing and adopting a filtering technique that ensures that the obtained autocorrelations are positive definite. Uncertainties are found by bootstrapping, choosing observed pairs of time-series with replacement. This is a non-parametric approach that can be used to explore the shapes of spatial autocorrelation functions. However, especially when the time-series overlap only partly in time it may represent an inefficient use of the available information.

Another approach is to consider each observed time-series (with n observations) as a point in the n -dimensional space and perform a principal component analysis (Fromentin *et al.* 1997; Kendall *et al.* 1999; Lekve *et al.* 1999; Viljugrein *et al.* 2001). This is typically a purely statistical approach which is difficult to interpret biologically. The conclusions derived from such analyses are also strongly dependent on the experimental design of data collection rather than the population dynamics as the method does not include spatial coordinates for the observations. Another problem is that the method is applicable only if the time span is the same for all time-series.

The present approach is based on the residuals obtained by fitting stochastic population models separately to each location. Ideally, these will be temporally independent, which is not generally the case for the yearly (log-) differences in population size as their distribution depends on population size in the previous year, which will generally be dependent between locations. Although our theoretical result on the scaling of residuals given in Appendix II is valid only for the homogeneous models used to derive it, it still probably provides the correct order of magnitude for how the spatial autocorrelation is affected by migration and autocorrelation in the noise. Because we use the full

likelihood for the complete data set, the method is statistically very efficient.

Earlier approaches do not make a distinction between demographic and environmental stochasticity. The models used are then based on the assumption that spatial autocorrelation only depends on the distance between locations and not on the population size. In the present approach, however, the effect of demographic stochasticity on the autocorrelation is incorporated into the model. Other approaches to this problem have always been based either on the assumption that the demographic variances are zero or that the population sizes are large enough to neglect demographic stochasticity. Even though large intraspecific variation may be found in $\hat{\sigma}_d^2$ (Sæther *et al.* 2003; Sæther *et al.* 2004), we have used a common estimate of σ_d^2 obtained from one location only. We consider this to be a more realistic approach giving more correct estimates of population synchrony than assuming $\sigma_d^2 = 0$. Furthermore, \hat{K} was larger than 1000 pairs in several of the colonies (Table 1), which makes the contribution from demographic stochasticity to the population fluctuations small (Lande *et al.* 2003). However, in cases where the local populations are small at some locations and larger at others, the effect of demographic variance may be considerable. In Fig. 4 we illustrate this strong effect of demographic stochasticity by plotting the estimated spatial autocorrelation functions for the residuals for different values of population size, using the estimated demographic variance and a value of demographic variance that is typical for birds (Sæther *et al.* 2004). We see that the synchrony decreases at a given distance with decreasing population size and increasing value of σ_d^2 .

During recent decades, the numbers of the continental great cormorant have increased over large parts of its distributional range (van Eerden & Gregersen 1995;

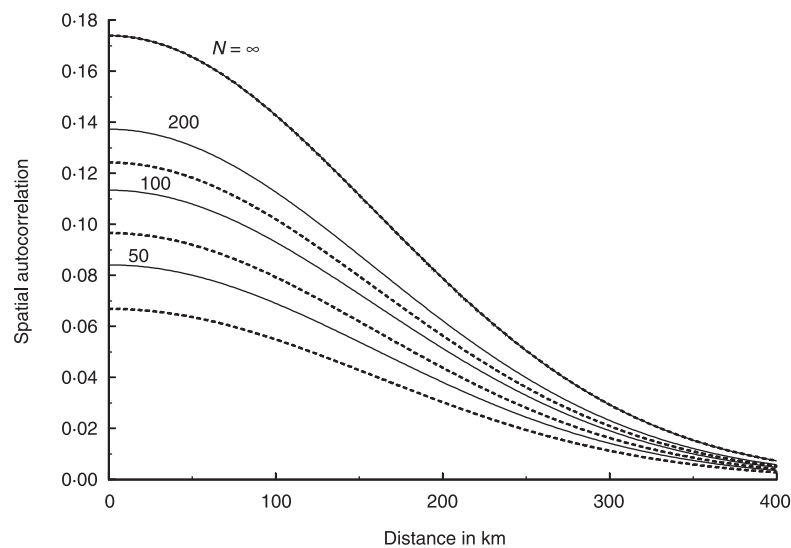


Fig. 4. The estimated spatial autocorrelation for the residuals (including demographic as well as environmental components) for different values of the population size. The autocorrelations are assumed to be of the Gaussian form, and the environmental variance $\sigma_e^2 = 0.005$, a typical value for local populations (Table 1), whereas the demographic variance is set equal to the estimated value $\hat{\sigma}_d^2 = 0.267$ (solid lines) and 0.4 (dotted lines).

Bregnballe *et al.* 2003), due mainly to reduced human persecution. As a consequence, an increasing number of new colonies have been established (Bregnballe & Rasmussen 2000), often involving a redistribution of individuals after years with poor breeding success (van Eerden & van Rijn 2003). Because of this pattern of colony formation, many colonies will fluctuate independently in size. However, the pattern of growth of most colonies is density-dependent (Frederiksen, Lebreton & Bregnballe 2001) and can be described well by a logistic model of density regulation (Table 1). By analysing the residuals from this model we are able to demonstrate large-scale synchrony in the population fluctuations of the continental great cormorant (Figs 2 and 3).

Theoretical analyses (summarized in Lande *et al.* 2003) as well as extensive simulation studies (e.g. Lundberg, Ranta & Kaitala 2000; Ranta *et al.* 2000) have shown that dispersal and spatial autocorrelations in the environmental noise both affect the spatial scaling of population synchrony. For the continental great cormorant, we estimate the spatial scale of population synchrony to be less than 300 km (Fig. 3). No quantitative analysis has yet been published on the pattern of dispersal of the great cormorant. However, high site fidelity has been found in some colonies (Schjørring *et al.* 2000). Furthermore, variation in NAO was able to explain nearly all the population synchrony at large distances (Fig. 2). Large population growth rates were also often associated with positive values of NAO (Table 1). As positive values of NAO in this area in general are associated with mild winters (Hurrell 1995), this suggests that variation in climate conditions in the wintering areas may act as a synchronizing agent on the population fluctuations of the continental great cormorant. As individuals from several colonies often use the same wintering areas (Marion 1995; Frederiksen *et al.* 2002) this may explain the synchronization effect of this large-scale climate phenomenon at large distances (Fig. 2). However, the tendency for a smaller synchronizing impact of NAO among closely located colonies (Fig. 2) may also suggest that other environmental conditions or dispersal is important at small distances.

Acknowledgements

This work was supported by the Norwegian Research Council (project 142883/432 and 155903/720, Klimaeffekt-programmet) and the US National Science Foundation. We also thank SOVON, the Staatliche Vogelschutzwarten, Landesumweltämter, H. Engström, W. Knief, M. R. van Eerden and H. Zimmermann for allowing us to include their data on colony sizes.

References

Bjørnstad, O.N. & Bolker, B. (2000) Canonical functions for dispersal-induced synchrony. *Proceedings of the Royal Society of London Series B*, **267**, 1787–1794.
 Bjørnstad, O.N., Ims, R.A. & Xavier, L. (1999b) Spatial population dynamics: analysing patterns and processes of

population synchrony. *Trends in Ecology and Evolution*, **14**, 427–432.
 Bjørnstad, O.N., Stenseth, N.C. & Saitoh, T. (1999a) Synchrony and scaling in dynamics of voles and mice in northern Japan. *Ecology*, **80**, 622–637.
 Bregnballe, T., Engström, H., Knief, W., van Eerden, M., van Rijn, S., Kieckbusch, J.J., Kieckbusch, J. & Eskildsen, J. (2003) Development of the breeding population of great cormorants (*Phalacrocorax carbo sinensis*) in the Netherlands, Germany, Denmark, and Sweden during the 1990s. *Vogelwelt*, **124** (Suppl.), 15–24.
 Bregnballe, T. & Rasmussen, T. (2000) Post-breeding dispersal of great cormorants *Phalacrocorax carbo sinensis* from Danish breeding colonies. *Dansk Ornitologisk Forenings Tidsskrift*, **94**, 175–187.
 Carss, D.E. & Ekins, G.R. (2002) Further European integration: mixed subspecies colonies of great cormorants *Phalacrocorax carbo* in Britain: colony establishment, diet, and implications for fisheries management. *Ardea*, **90**, 23–41.
 Catchpole, E.A., Morgan, B.J.T., Coulson, T.N., Freeman, S.N. & Albon, S.D. (2000) Factors influencing Soay sheep survival. *Applied Statistics*, **49**, 453–472.
 Cattadori, I.M., Merler, S. & Hudson, P.J. (2000) Searching for mechanisms of synchrony in spatially structured gamebird populations. *Journal of Animal Ecology*, **69**, 620–638.
 Drinkwater, K.F., Belgrano, A., Borja, A., Conversi, A., Edwards, M., Greene, C.H., Ottersen, G., Pershing, A.J. & Walker, K. (2003) The response of marine ecosystems to climate variability associated with the North Atlantic Oscillation. *The North Atlantic Oscillation. Climatic Significance and Environmental Impact* (eds J.W. Hurrell, Y. Kushnir, G. Ottersen & M. Visbeck), pp. 211–234. American Geophysical Union, Washington.
 Efron, B. & Tibshirani, R.J. (1993) *An Introduction to the Bootstrap*. Chapman & Hall, New York.
 Elton, C.S. (1924) Periodic fluctuations in the number of animals: their causes and effects. *British Journal of Experimental Biology*, **2**, 119–163.
 Engen, S. (2001) A dynamic and spatial model with migration generating the log-Gaussian field of population densities. *Mathematical Biosciences*, **173**, 85–102.
 Engen, S., Bakke, Ø. & Islam, A. (1998) Demographic and environmental stochasticity – concepts and definitions. *Biometrics*, **54**, 840–846.
 Engen, S., Lande, R. & Sæther, B.-E. (2002a) Migration and spatio-temporal variation in population dynamics in a heterogeneous environment. *Ecology*, **83**, 570–579.
 Engen, S., Lande, R. & Sæther, B.-E. (2002b) The spatial scale of population fluctuations and quasi-extinction risk. *American Naturalist*, **160**, 439–451.
 Engen, S., Lande, R., Sæther, B.-E. & Weimerskirch, H. (2005) Extinction in relation to demographic and environmental stochasticity in age-structured models. *Mathematical Biosciences*, **195**, 210–227.
 Frederiksen, M. & Bregnballe, T. (2000) Diagnosing the decline in return rate of 1-year-old cormorants: mortality, emigration or delayed return? *Journal of Animal Ecology*, **69**, 753–761.
 Frederiksen, M. & Bregnballe, T. (2001) Conspecific reproductive success affects age of recruitment in a great cormorant, *Phalacrocorax carbo sinensis*, colony. *Proceedings of the Royal Society of London of London Series B*, **268**, 1519–1526.
 Frederiksen, M., Bregnballe, T., van Eerden, M.R., van Rijn, S. & Lebreton, J.D. (2002) Site fidelity at wintering cormorants *Phalacrocorax carbo sinensis* in Europe. *Wildlife Biology*, **8**, 241–250.
 Frederiksen, M., Lebreton, J.D. & Bregnballe, T. (2001) The interplay between culling and density-dependence in the great cormorant: a modelling approach. *Journal of Applied Ecology*, **38**, 617–627.

- Fromentin, J.-M., Stenseth, N.C., Gjøsæther, J., Bjørnstad, O.N., Falck, W. & Johannesen, T. (1997) Spatial patterns of the temporal dynamics of three gadoid species along the Norwegian Skagerrak coast. *Marine Ecology Progress Series*, **155**, 209–222.
- Grenfell, B.T., Wilson, K., Fikenstadt, B.F., Coulson, T.N., Murray, S., Albon, S.D., Pemberton, J.M., Clutton-Brock, T.H. & Crawley, M.J. (1998) Noise and determinism in synchronized sheep dynamics. *Nature*, **394**, 674–677.
- Hurrell, J.W. (1995) Decadal trends in the North Atlantic Oscillation: regional temperatures and precipitation. *Science*, **269**, 676–679.
- Hurrell, J.W., Kushnir, Y., Ottersen, G. & Visbeck, M. (2003) An overview of the North Atlantic Oscillation. *The North Atlantic Oscillation. Climatic Significance and Environmental Impact* (eds J.W. Hurrell, Y. Kushnir, G. Ottersen & M. Visbeck), pp. 1–35. American Geophysical Union, Washington.
- Karlin, S. & Taylor, H.M. (1981) *A Second Course in Stochastic Processes*. Academic Press, New York.
- Kendall, B.E., Briggs, C.J., Murdoch, W.W., Turchin, P., Ellner, S.P., McCauley, E., Nisbet, R.M. & Wood, S.N. (1999) Why do populations cycle? A synthesis of statistical and mechanistic modelling approaches. *Ecology*, **80**, 1789–1805.
- Kendall, B.E., Bjørnstad, O.N., Bascompte, J., Keitt, T.H. & Fagan, W.F. (2000) Dispersal, environmental correlation, and spatial synchrony in population dynamics. *American Naturalist*, **155**, 628–636.
- Koenig, W. (1999) Spatial autocorrelation in ecological phenomena. *Trends in Ecology and Evolution*, **14**, 22–26.
- Lande, R., Engen, S. & Sæther, B.-E. (1999) Spatial scale of population synchrony: environmental correlation versus dispersal and density regulation. *American Naturalist*, **154**, 271–281.
- Lande, R., Engen, S. & Sæther, B.-E. (2003) *Stochastic Population Dynamics in Ecology and Conservation*. Oxford University Press, Oxford.
- Lande, R. & Orzack, S.H. (1988) Extinction dynamics of age-structured populations in a fluctuating environment. *Proceedings of the National Academy of Sciences USA*, **85**, 7418–7421.
- Lekve, K., Stenseth, N.C., Gjøsæther, J., Fromentin, J.-M. & Gray, J.S. (1999) Spatio-temporal patterns in diversity of a fish assemblage along the Norwegian Skagerrak coast. *Marine Ecology Progress Series*, **178**, 17–27.
- Lindström, J., Ranta, E. & Lindén, H. (1996) Large-scale synchrony in the dynamics of capercaillie, black grouse and hazel grouse populations in Finland. *Oikos*, **76**, 221–227.
- Lundberg, P., Ranta, E. & Kaitala, V. (2000) Population variability in space and time. *Trends in Ecology and Evolution*, **15**, 460–464.
- Marion, L. (1995) Where two species meet: origin, habitat at choice and niche segregation of cormorants *Phalacrocorax c. carbo* and *P. c. sinensis* in the common wintering area (France), in relation to breeding isolation in Europe. *Ardea*, **83**, 103–114.
- May, R.M. (1973) Stability in randomly fluctuating versus deterministic environments. *American Naturalist*, **107**, 621–650.
- May, R.M. (1974) *Stability and Complexity in Model Ecosystems*, 2nd edn. Princeton University Press, Princeton.
- Moran, P.A.P. (1953) The statistical analysis of the Canadian lynx cycle. II. Synchronization and meteorology. *Australian Journal of Zoology*, **1**, 281–298.
- Mysterud, A., Yoccoz, N.G., Stenseth, N.C. & Langvatn, R. (2000) Relationships between sex ratio, climate and density in red deer: the importance of spatial scale. *Journal of Animal Ecology*, **69**, 959–974.
- Ottersen, G., Planque, B., Belgrano, A., Post, E., Reid, P.C. & Stenseth, N.C. (2001) Ecological effects of the North Atlantic Oscillation. *Oecologia*, **128**, 1–14.
- Paradis, E., Baillie, S.R., Sutherland, W.J. & Gregory, R.D. (1999) Dispersal and spatial scale affect synchrony in spatial population dynamics. *Ecology Letters*, **2**, 114–120.
- Paradis, E., Baillie, S.R., Sutherland, W.J. & Gregory, R.D. (2000) Spatial synchrony in populations of birds: effects of habitat, population trend, and spatial scale. *Ecology*, **81**, 2112–2125.
- Peltonen, M., Liebhold, A.M., Bjørnstad, O.N. & Williams, D.W. (2002) Spatial synchrony in forest insect outbreaks: roles of regional stochasticity and dispersal. *Ecology*, **83**, 3120–3129.
- Ranta, E., Kaitala, V. & Lundberg, P. (1997b) The spatial dimension in population fluctuations. *Science*, **278**, 1621–1623.
- Ranta, E., Lindström, J. & Helle, E. (1997a) The Moran effect and synchrony in population dynamics. *Oikos*, **78**, 136–142.
- Ranta, E., Lundberg, P., Kaitala, V. & Laakso, J. (2000) Visibility of the environmental noise modulating population dynamics. *Proceedings of the Royal Society of London Series B*, **267**, 1851–1856.
- Ripa, J. (2000) Analyzing the Moran effect and dispersal: their significance and interaction in synchronous population dynamics. *Oikos*, **89**, 175–187.
- Ripley, B.D. (1987) *Stochastic Simulation*. John Wiley & Sons, New York.
- Sæther, B.-E., Engen, S., Islam, A., McCleery, R. & Perrins, C. (1998) Environmental stochasticity and extinction risk in a population of a small song bird, the great tit. *American Naturalist*, **151**, 441–450.
- Sæther, B.-E., Engen, S., Møller, A.P., Matthysen, E., Adriaensens, F., Fiedler, W., Leivits, A., Lambrechts, M.M., Visser, M.E., Anker-Nilssen, T., Both, C., Dhondt, A.A., McCleery, R.H., McMeeking, J., Potti, J., Røstad, O.W. & Thomson, D. (2003) Climate variation and regional gradients in population dynamics of two hole nesting passerines. *Proceedings of the Royal Society of London Series B*, **270**, 2397–2404.
- Sæther, B.-E., Engen, S., Møller, A.P., Weimerskirch, H., Visser, M.E., Fiedler, W., Matthysen, E., Lambrechts, M.M., Badyaev, A., Becker, P.H., Brommer, J.E., Bukacinski, D., Bukacinska, M., Christensen, H., Dickinson, J., du Feu, C., Gehlbach, F.R., Heg, D., Hötker, H., Merilä, J., Nielsen, J.T., Rendell, W., Thomson, D.L., Török, J. & Van Hecke, P. (2004) Life history variation predicts the effects of demographic stochasticity on avian population dynamics. *American Naturalist*, **164**, 793–802.
- Schjørring, S., Gregersen, J. & Bregnballe, T. (2000) Sex difference in criteria determining fidelity towards breeding sites in the great cormorant. *Journal of Animal Ecology*, **69**, 214–223.
- Stenseth, N.C., Chan, K.S., Tong, H., Boonstra, R., Boutin, S., Krebs, C.J., Post, E., O'Donoghue, M., Yoccoz, N.G., Forchhammer, M.C. & Hurrell, J.W. (1999) Common dynamic structure of Canada lynx populations within three climatic regions. *Science*, **285**, 1071–1073.
- Stenseth, N.C., Mysterud, A., Ottersen, G., Hurrell, J.W., Chan, K.S. & Lima, M. (2002) Ecological effects of climate fluctuations. *Science*, **297**, 1292–1296.
- Tuljapurkar, S.D. (1982) Population dynamics in variable environments. III. Evolutionary dynamics of r-selection. *Theoretical Population Biology*, **21**, 114–140.
- Turelli, M. (1977) Random environments and stochastic calculus. *Theoretical Population Biology*, **12**, 140–178.
- Van Eerden, R.M. & Gregersen, J. (1995) Long-term changes in the northwest European population of cormorants *Phalacrocorax carbo sinensis*. *Ardea*, **83**, 61–79.
- Van Eerden, R.M., Koffijberg, K. & Platteeuw, M. (1995) Riding on the crest of the wave: possibilities and limitations for a thriving population of migratory cormorants *Phalacrocorax carbo* in man-dominated wetlands. *Ardea*, **83**, 1–9.
- Van Eerden, R.M. & van Rijn, S. (2003) Redistribution of cormorant population in the IJsselmeer area. *Cormorant Research Group Bulletin*, **5**, 33–37.

Viljugrein, H., Lingjærde, O.C., Stenseth, N.C. & Boyce, M.C. (2001) Spatiotemporal patterns of mink and muskrat in Canada during a quarter century. *Journal of Animal Ecology*, **70**, 671–682.
Visbeck, M.H., Hurrell, J.W., Polvani, L. & Cullen, H.M.

(2001) The North Atlantic Oscillation: past, present, and future. *Proceedings of the National Academy of Sciences USA*, **98**, 12876–12877.

Received 20 February 2004; accepted 25 September 2004

Appendix I

LIKELIHOOD AND SIMULATIONS FOR THE MULTINORMAL DISTRIBUTION

Using Cholesky decomposition

Let (X_1, X_2, \dots, X_n) be multnormally distributed with mean values $EX_i = \mu_i$, $\text{var}(X_i) = \sigma_i^2$ and correlations $\text{corr}(X_i, X_j) = \rho_{ij}$ and write $Y_i = (X_i - \mu_i)/\sigma_i$ for the standardized components. The Y_i can be expressed as linear combinations of independent standardized normal variates U_1, U_2, \dots, U_n

$$Y_i = \sum_{j=1}^i a_{ij} U_j \tag{eqn 12}$$

where the coefficients a_{ij} defining a lower triangular matrix are determined by the correlation matrix only (Ripley 1987). Using the fact that $\text{corr}(Y_i, Y_j) = \text{corr}(X_i, X_j) = \rho_{ij}$ and writing up the correlations in terms of the a_{ij} we can easily solve for these coefficients. We first observe that $a_{11} = 1$ and subsequently for $i = 2, 3, \dots, n$ the coefficients with i as first index are:

$$a_{i1} = \rho_{i1}$$

$$a_{ij} = \left(\rho_{ij} - \sum_{k=1}^{i-1} a_{ik} a_{jk} \right) / a_{jj} \quad \text{for } j = 1, 2, \dots, i-1.$$

$$a_{ii} = \left(1 - \sum_{j=1}^{i-1} a_{ij}^2 \right)^{1/2}.$$

Stochastic simulation can now be performed by first simulating the U_i , then calculating the Y_i using eqn 12, and finally computing the $X_i = \sigma_i Y_i + \mu_i$.

To find the likelihood function we need the distribution of the X_i which can be expressed as:

$$f(X_1, X_2, \dots, X_n) = \prod_{i=1}^n \phi(U_i) / (|a_{ii}| \sigma_i)$$

where $\phi(u) = (2\pi)^{-1/2} \exp(-u^2/2)$ is the standard normal distribution. Here the observations X_i are the given data and the independent standardized variables U_i must be calculated by first calculating the $Y_i = \sigma_i X_i + \mu_i$ and solving eqn 12 giving:

$$U_1 = Y_1/a_{11}$$

and subsequently for $i = 2, 3, \dots, n$,

$$U_i = \left(Y_i - \sum_{j=1}^{i-1} a_{ij} U_j \right) / a_{ii}.$$

The contribution to the log likelihood from the vector (X_1, X_2, \dots, X_n) , defined as a function of the unknown parameters to be estimated, is:

$$\ln L = -\sum_{i=1}^n \left[\frac{1}{2} U_i^2 + \ln(\sigma_i) + \ln(|a_{ii}|) \right].$$

Finally, the contributions from all independent vectors of observed residuals through time are added to produce the complete likelihood function.

Appendix II

SPATIAL SCALING IN THE LOGLINEAR MODEL

The following is based on the linear model with migration dealt with by Engen (2001) and later applied to derive several scaling results (Engen *et al.* 2002a,b). In the absence of migration and demographic stochasticity we consider the loglinear continuous time model:

$$dn(z, t) = [r - \gamma n(z, t)]n(z, t)dt + n(z, t)\sigma_e dB_e(z, t)$$

where $n(z, t)$ is the population size at location z at time t , r is the population growth rate at small densities, and γ is the strength of local density regulation. The derivative $(d/dt)B(z, t)$ is a white noise process at location z with no temporal autocorrelation, actually the derivative of a Brownian motion (Karlin & Taylor 1981). This environmental noise has a spatial autocorrelation, called the spatial environmental autocorrelation, defined by $\rho_e(z)dt = E dB_e(w, t)dB_e(w + z, t)$.

Adding density-independent migration to this model the equation for the densities takes the form:

$$dn(z, t) = [r - \gamma n(z, t)]n(z, t) + m \int [n(z + \xi, t) - n(z, t)] dp(\xi) d\xi + \sigma_e n(z, t) dB_e(z, t),$$

giving for the log densities:

$$dX(z, t) = [r_0 - \gamma X(z, t)]dt + mdt \int [e^{X(z+\xi, t) - X(z, t)} - 1] p(\xi) dr + \sigma_e dB_e(z, t),$$

where $r_0 = r - 1/2 \sigma_e^2$ is the stochastic growth rate. Here individuals are assumed to migrate at a rate m and the migration distance has distribution $p(\xi)$ with zero mean. In the limit as m tends to infinity and the migration distance tends to zero one can show that the Fourier transform of the autocovariance function $c(z, t) = \text{cov}[X(w, u), X(w + z, u + t)]$, that is

$$f_i(\omega_1, \omega_2) = \int \exp[-i(\omega_1 z_1 + \omega_2 z_2)] c(z_1, z_2, t) dz_1 dz_2,$$

takes the form:

$$f_i(\omega_1, \omega_2) = \frac{f_e(\omega_1, \omega_2)}{2\gamma + M(\omega_1^2 + \omega_2^2)} e^{-[\gamma + \frac{1}{2} M(\omega_1^2 + \omega_2^2)]t},$$

where f_e is the Fourier transform of $\sigma_e^2 \rho_e(z)$ (Engen 2001). In the limit the migration of each individual is described by a two-dimensional Brownian motion with zero mean. The parameter M is easily interpreted through the fact that the probability that an individual migrates a distance longer than d during a time interval of length t is $\exp[-d^2/(2Mt)]$.

We now want to investigate the spatial scaling of the residuals obtained by considering the continuous model only at discrete times with time steps one, that is:

$$R(z, t) = [X(z, t+1) - X(z, t)] - [r_0 - \gamma X(z, t)]$$

which has covariance function

$$\begin{aligned} c_R(z) &= \text{cov}[R(w, t), R(w+z, t)] \\ &= [1 + (1 - \gamma)^2]c(z, 0) - 2(1 - \gamma)c(z, 1). \end{aligned}$$

The Fourier transform of $c_R(z)$ is

$$g_R(\omega_1, \omega_2) = [1 + (1 - \gamma)^2]f_0(\omega_1, \omega_2) - 2(1 - \gamma)f_1(\omega_1, \omega_2).$$

Following Engen *et al.* (2002b) we can find the square of the spatial scaling of $c_R(z)$, which is the variance

along one direction of the covariance function scaled to become a distribution, as:

$$l_R^2 = \left[-\frac{\partial^2 g_R(\omega_1, \omega_2)}{\partial \omega_1^2} g_R(0, 0) \right]_{\omega_1=\omega_2=0}.$$

This leads to the spatial scaling:

$$l_R^2 = l_e^2 + M \left\{ 1/\gamma - \frac{2(1 - \gamma)}{[1 + (1 - \gamma)^2]e^\gamma - 2(1 - \gamma)} \right\}.$$

Numerical calculations shows that the coefficient of M is within 5% from 1 for $0 < \gamma < 1.15$ which covers most typical values for the density regulation. Hence:

$$l_R^2 \approx l_e^2 + M.$$

Writing \bar{d} for the root mean square of the migration

distance for one season, that is, $\bar{d} = \int_0^\infty \frac{u^2}{2m} e^{-\frac{u^2}{2m}} du = \sqrt{\pi m/2}$

(Engen 2001), giving $M = 2\bar{d}^2/\pi$, the scaling result takes the form:

$$l_R^2 \approx l_e^2 + 2\bar{d}^2/\pi \approx l_e^2 + 0.64\bar{d}^2.$$